論文 10-2-18

大變形을 가지는 四角形 薄形유리板의 非線形 差分解析

A Finite Difference Large Displacement Analysis of Rectangular Thin Glass Plate

김 치 경*
Chi-Kyung Kim

ABSTRACT

A new approach to the analysis of thin. rectangular window giass glass supported on flexible gaskets, and subjected to uniform lateral pressures was evolved. Based on the Von Karman theory of plates and using the finite difference method. a computer program which determines the deflections and stresses in simply supported thin glass plates was developed.

요 약

均等한 縱方向 壓力을 받고있는 柔軟性 物質인 게스킷 上의 얇은 四角形유리板을 새로운 接近方法으로 解析하였다. 본-카만의 板의 理論에 依거 單純支持의 얇은 유리板의 應力과 처짐을 差分法으로 解析하였으며 非線形的으로 計算되는 컴퓨터 프로그램을 發展시켰다. 解의 보다 빠른 收斂을 위한 새로운 反復法을 展開시켰다.

1. Introduction

Glass plates are widely used in modern buildings. With larger and larger sizes of glass plates being used in high-rise buildings, it is becoming important to be able to predict accurately the response of glass plates under lateral loads representing wind pressure. The first significant analysis of thin plates was accomplished in the early 1800s by Cauchy, Poisson, Navier and Kirchhoff. The research done by these pioneers was very significant, and many of the techniques which they developed are used in engineering analysis today. A nonlinear plate theoy was first

* 인천대학교 산업안전공학과

developed by Von Karman in 1910. He coupled the effects of in-plane force with out-of-plane deflections. Closed form solutions for his theory, even for simple rectangular plates, are not known. Early investigators obtained only approximate solutions by using variational methods[4]. However, in the last 30 years, which the help of the digital computer, methods such as finite differences and finite elements have become practical. Subsquent developments in the field of laterally loaded, thin rectangular plates with large deflections are well documented elsewhere[2,5].

2. Theoretical Model

This section provides a brief description of the model, which was employed as part of the reseach plan to provide prediction of stresses and displacements in monolithic glass plates units.

2.1 Theory

A simply supported glass plate under lateral pressure sustains deflections which are small in comparison to the in-plane dimensions of the plate, but are of the same order of magnitude as the plate thickness. Hence, the analysis may be classified as "small strain, large displacement". Because of the relatively large out-of-plane displacements, the analysis becomes geometrically nonlinear. This geometric nonlinearity requires that both membrane and bending stresses be included in the analysis. The theoretical model uses Von Karman's theory of nonlinear plate analysis to characterize the small strain, large displacement behavior of a nonlinear plate are :

$$D\nabla^4 W = Q + tL(W,F) \quad \cdots\cdots (1)$$

and

$$\nabla^4 F = -\frac{E}{2} L(W,W) \quad \cdots\cdots (2)$$

where :

D =flexural rigidity of the plate
$=Et^3/12(1-\nu^2)$

W =lateral deflection

F =Airy stress function

Q =lateral pressure

t =plate thickness

E =Young's modulus of elesticity

ν =Poisson's ratio

∇^4 =the biharmonic operator

$$= \frac{\partial^4}{\partial x^4} + \frac{\partial^4}{\partial x^2 \partial y^2} + \frac{\partial^4}{\partial y^4}$$

$$L(W,F) = \frac{\partial^2 W}{\partial x^2}\frac{\partial^2 F}{\partial y^2} - 2\frac{\partial^2 W}{\partial x \partial y}\frac{\partial^2 F}{\partial x \partial y} + \frac{\partial^2 W}{\partial y^2}\frac{\partial^2 F}{\partial x^2}$$

The Airy stress function F defines membrane stresses such that

$$\sigma_x = \frac{\partial^2 F}{\partial y^2}, \quad \sigma_y = \frac{\partial^2 F}{\partial x^2}, \quad \tau_{xy} = \frac{\partial^2 F}{\partial x \partial y} \quad \cdots\cdots (3)$$

Bending stresses can be calculated from :

$$\sigma^b{}_x = \pm\frac{6M_x}{t^2}, \quad \sigma^b{}_y = \pm\frac{6M_y}{t^2}, \quad \tau^b{}_{xy} = \pm\frac{6M_{xy}}{t^2} \quad \cdots\cdots (4)$$

where

$$M_x = -D\left(\frac{\partial^2 W}{\partial x^2} + \nu\frac{\partial^2 W}{\partial y^2}\right)$$

$$M_y = -D\left(\frac{\partial^2 W}{\partial y^2} + \nu\frac{\partial^2 W}{\partial x^2}\right)$$

$$M_{xy} = -D(1-\nu)\frac{\partial^2 W}{\partial x \partial y}$$

Using the coordinate system defined in Figure 2, boundary conditions for a thin, simply supported glass plate can be represented as follows :

(1) Flexural boundary conditions :

$$W=0,\ M_x=0,\ \frac{\partial^2 W}{\partial x^2}=0 \text{ at } x=\frac{a}{2}$$

$$W=0,\ M_y=0,\ \frac{\partial^2 W}{\partial y^2}=0 \text{ at } y=\frac{b}{2} \quad \cdots\cdots (5)$$

$$\frac{\partial W}{\partial x}=0 \text{ at } x=0$$

$$\frac{\partial W}{\partial y}=0 \text{ at } y=0$$

(2) Membrane boundary conditions :

$$\sigma_x=\frac{\partial^2 F}{\partial y^2}=0;\quad \tau_{xy}=-\frac{\partial^2 F}{\partial x\partial y}=0 \text{ at } x=\frac{a}{2}$$

$$\sigma_y=\frac{\partial^2 F}{\partial x^2}=0;\quad \tau_{xy}=-\frac{\partial^2 F}{\partial x\partial y}=0 \text{ at } y=\frac{b}{2} \quad \cdots\cdots (6)$$

Figure 3 illustrates these boundary conditions.

2.2 Solution of Von Karman's Equations

Solution of Von Karman's equations employed the finite difference method. The biharmonic operator can be reperesented by a molecule using the central difference formula, which can be found in a text book on the finite difference model(Crandall, 1956). Figure 4 illustrates the biharmonic operator and the second derivative in central difference form. Von Karman's nonlinear Equation(1), (2) can be represented by two algebraic functions, using the

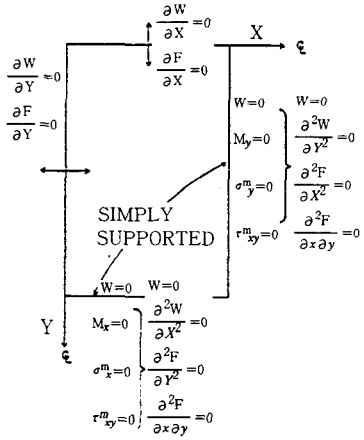

Fig. 1 Boundary conditions for simply supported thin plate

two central difference equations. Equation 1 becomes :

$$[C](W)=Q+(f_1(W,F)) \quad \cdots\cdots (7)$$

and Equation 2 becomes

$$[D](F)=(f_2(W)) \quad \cdots\cdots (8)$$

where

[A] and [B]=Biharmonic operators

W=vector representing lateral displacement

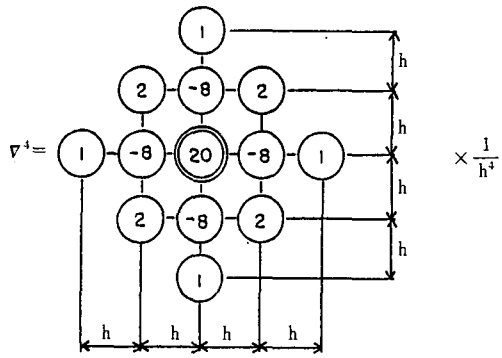

a) Biharmonic Operator in central difference form

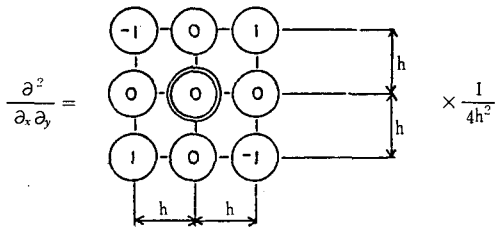

b) Second derivative in central difference operator

Fig. 2 Two-dimensional finite difference operator

Q=vector representing load

F=vector representing Airy function

f_1 and f_2=nonlinear functions representing part of right side of Von Karman's equations.

It can be seen that Equation 7 represents lateral deflection, while Equation 8 represents the Airy stress function. One of the major advantages of the finite difference solution can now be illustrated. Both matrices [A] and [B] are positive definite and symmetric, and can therefore be decomposed by Cholesky decomposition into U'DU where U is an upper triangular matrix and D is a diagonal matrix. The matrices are then coded by the computer in half bandwidths. This step is only done once in the beginning of the solution, and the banded matrices are then used throughout the iterations loading leading to the solution of the W and F vectors. Like any other iterative technique, new values for the variables(in this case W and F) are

calculated based on values obtained from the previous iteration the f_1 function can be calculated numerically from the expression for L(W, F). The first Von Karman's equation for the (n+1)-th iteration becomes

$$[C](W^{n+1})=(Q)+(f_1(W^n, F^n)) \quad \cdots\cdots (9)$$
$$=(R_1)$$

From this, W^{n+1} can be determined. Now that W^{n+1} is known, it can be substitute into the right hand side of the second Von Karman equation such that Equation 8 becomes

$$[D](F^{n+1})=(f_2(W^{n+1})) \quad \cdots\cdots (10)$$
$$=(R_2)$$

and from this F^{n+1} can be obtained.

Efficient iterative techniques using nonlinear interpolation factors has been developed to reduce computer time and to assure convergence. A so-called relaxation parameter has been introduced, such that

$$F^{n+1}=(1-\lambda)F^n+\lambda F^{n+1} \quad \cdots\cdots (11)$$

and

$$\overline{W}^{n+1}=(1-\mu)W^n+\mu W^{n+1} \quad \cdots\cdots (12)$$

The parameter λ and μ have been optimized by numerical experimentation with different aspect ratios of plates such that

$$\lambda=1/2$$

and

$$\mu=0.8/(W-1)-0.004W \text{ for } W\geq 1.8 \quad \cdots\cdots (13)$$
$$\mu=1-W/9 \text{ for } W\leq 1.8 \quad \cdots\cdots (14)$$

where

$$W=W^n_{max}/t$$

An error term is used to end the iteration when convergence is reached in the computation of W :

$$\varepsilon^{n+1}=\sum_{j=1}^{N} | W^{n+1}_j-W^n_j | /N\leq \rho(W_{max})^{n+1} \quad (15)$$

where

n =iteration number

j =node number

N =number of nodes in the grid

ρ =iterative tolerance number, usually 0.001

From experience, it has been determined that convergence is reached in approximately 10-20 iterations.

3. Example Problem

The example is a simply supported uniformly loaded square plate having boundary conditions as mentioned above. The dimensions and material properties of the plate are given as follows

a =10in

b =10in

t =0.04in

E =10000000psi

ν =0.316

The plate is subjected to a uniformly increasing static load up to 0.83psi. Because of the double symmetry of the plate, only one quarter of the plate is used in the model. In Figure 3, the effect of the fine mesh on the maximum deflection of the plate is shown. The convergence of the deflection improves as number of mesh points is increased. The effect of the grid size on the bending stresses at the corners of the plate is as shown in Figure 4. These stress curves appear to converge as the grid size become small. This is also true for the membrane stresses at the center of the edge of the plate. The difference between the finite difference solution and the finite element solution is small(as shown by the curves in Figure 4 and Figure 5); thus, it is unnecessary to carry the analysis further

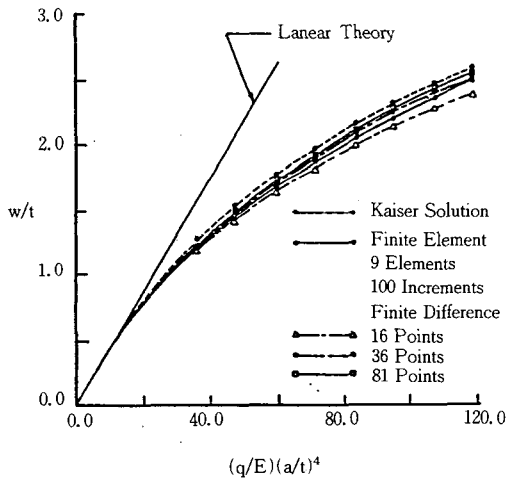

Fig. 3 Effect of mesh size on maximum deflection

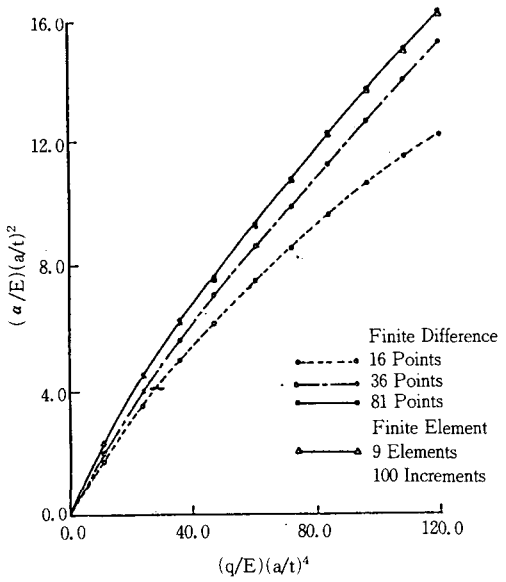

Fig. 4 Effect of mesh size on bending stresses at the corner

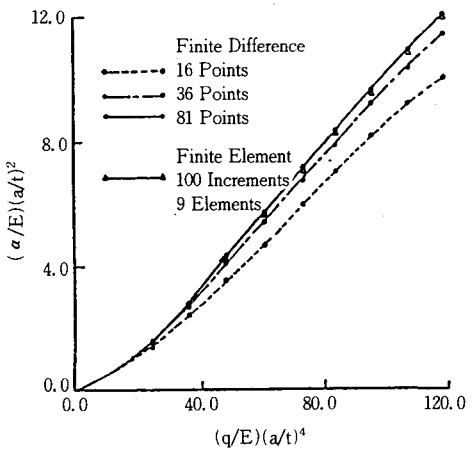

Fig. 5 Effect of mesh size on membrane stresses along the center edge

by refinig the mesh size to obtain results that match Al-Tayyib's solution point by point. According to Figure 3 through 5, we can state briefly that deflections and stresses approach the exact solution from a lower bound as the mesh size is reduced.

4. Conclusions

The following conclusions are advanced :

1) the results from the model developed agree well previous solutions,
2) the model developed is very efficient in computer storage requirements and excusion time,
3) The results obtained are more accurate than Kaiser's solution, because for every loading, the iteration converged exactly to the Von Karman field equations,
4) variable mesh size allows analysis of any size of rectangular plate.

References

1) D. C. Anians, Experimemental Study of Edge Displacements of Laterally Loaded Window Glass Plates, Master Thesis, Texas Tech University, p. 166, 1979.
2) R. Szilard, Theory and Analysis of Plates, Classical and Numerical Methods, Prentice-Hall, INC. Englewood Cliff, New Jersey, 1974.
3) S. Levy, Bending of Rectangular Plates with Large Deflections, NACA, TN No. 846, 1942.
4) D. McFarland, B. L. Smith, and W. D. Bernhart, Analysis of Plates, Spartan Books, New York, 1972.
5) A. C. Ugural, Stresses in Plates and Shells, McGraw-Hill Book Company, New York, 1982.